IEEE Access
Multidisciplinary | Rapid Review | Open Access Journal

Received May 21, 2019, accepted June 9, 2019, date of publication June 17, 2019, date of current version September 4, 2019.

Digital Object Identifier 10.1109/ACCESS.2019.2923264

Electromagnetic Force Distribution and Deformation Homogeneity of Electromagnetic Tube Expansion With a New Concave Coil Structure

LI QIU[1,2], (Member, IEEE), YANTAO LI[1], YIJIE YU[3], A. ABU-SIADA[4], (Senior Member, IEEE), QI XIONG[1], (Member, IEEE), XIAOXIANG LI[5], LIANG LI[5], PAN SU[1], AND QUANLIANG CAO[5]

[1]College of Electrical Engineering and New Energy, China Three Gorges University, Yichang 443002, China
[2]Hubei Key Laboratory of Cascaded Hydropower Stations Operation and Control, China Three Gorges University, Yichang 443002, China
[3]State Grid Putian Electric Supply Company, Putian 351100, China
[4]Department of Electrical and Computer Engineering, Curtin University, Perth, WA 6102, Australia
[5]Wuhan National High Magnetic Field Center, Huazhong University of Science and Technology, Wuhan 430074, China

Corresponding authors: Pan Su (supan_ctgu@163.com) and Quanliang Cao (quanliangcao@hust.edu.cn)

This work was supported in part by the National Natural Science Foundation of China under Grant 51877122 and Grant 51707104, and in part by the Research Fund for Excellent Dissertation of China Three Gorges University under Grant 2019SSPY065.

ABSTRACT In the conventional electromagnetic tube expansion, the end effects generated by the conventional helix coil may lead to inhomogeneous tube deformation in the axial direction. This paper is aimed at overcoming this issue by proposing a new concave coil structure to replace the helix coil currently used by the industry practice to generate a radial electromagnetic force on the tube. The proposed concave coil is expected to reinforce the electromagnetic force distribution profile and, hence, improving the axial inhomogeneous deformation of the tube. In this context, a new R-L criterion of deformation uniformity is first proposed. Second, an electromagnetic-structural coupling finite element model is established to investigate the relationship between the distribution of electromagnetic force generated by the concave coil and the uniformity of the tube under various voltage levels. The effectiveness of the proposed method is validated through a series of experimental and simulation analyses. Furthermore, based on the characteristics of the electromagnetic tube expansion, a modified multilayer concave coil structure is proposed to overcome the axial inhomogeneous deformation of long tubes.

INDEX TERMS Concave coil, deformation homogeneity, electromagnetic force distribution, electromagnetic tube expansion.

I. INTRODUCTION

Light alloys have been given much attention in the last few years due to its wide applications in various industry fields such as aerospace, transportation, and machinery. Owing to the fact that wrinkling and spring back are easily occurred during conventional forming process at room temperature, electromagnetic forming (EMF) has been widely adopted to improve the plastic deformation ability of materials and light alloys [1].

According to the nature of the workpiece, EMF can be categorized into electromagnetic sheet forming and electromagnetic tube forming. In electromagnetic sheet forming, the electromagnetic force generated by a spiral coil is mainly in axial direction. This electromagnetic force is not homogenous along the entire workpiece as the radial force component at the center is higher than the force at the sheet edges which results in a poor forming performance in radial direction. On the other hand, the electromagnetic force generated by a helix coil in electromagnetic tube forming is mainly in radial direction with a higher component on the central area than the edges of the tube. This leads to inhomogeneous distributed electromagnetic forces in the axial direction. As a result of this inhomogeneous force distribution, a significant reduction of the workpiece thickness occurs in the central area compared to the thickness of the edges and

The associate editor coordinating the review of this manuscript and approving it for publication was Mohamed Kheir.

it will be easy to crack [2]–[4]. As such, obtaining a homogeneous forming effect has become one of the main goals of many scholars in the electromagnetic forming research field.

To improve sheet uneven forming performance, Kamal and Daehn have developed a uniform pressure actuator based on the principle of electromagnetic tube expansion that can produce a uniform electromagnetic force on the sheet [5]. This uniform pressure actuator has significantly improved the forming effect compared with conventional electromagnetic sheet forming and has been widely used in several industry and research fields including Embossing Forming of Battery Fuel Plate [6], cell phone shell fine forming [7] and electromagnetic welding [8]. Tekkaya et al. designed a driving coil to generate electromagnetic force that varies with the contour of the sheet to improve the forming performance [9]. Ahmed et al. proposed a design of a flat coil of a variable cross section to produce a better electromagnetic force distribution over the workpiece [10]. An Electromagnetic Forming with a Local Loading method was proposed to reduce the electromagnetic force at the central region of the workpiece. This method achieved a well-proportioned deformation at the edges of the workpiece [11]. A new dynamic forming method named Lorentz-force-driven sheet metal stamping was proposed by Cao et al. in which the shape of the workpiece can be well controlled [12].

To improve the homogeneous forming performance of a tube, a small coil is proposed to be placed at different locations of the aluminum alloy tube [13]. Through applying field shaper in the electromagnetic compression [14], and electromagnetic welding [15], the magnetic flux density and electromagnetic force generated are becoming more uniform. Qiu adopted three coils which are placed at the middle and both ends of the tube to generate uniform axial electromagnetic force that can reduce the wall thickness at the central area of the tube [16]. A coupled electromagnetic-mechanical numerical model was developed using ANSYS software to analyze the main factors affecting the tube forming uniformity. Li et al. analyzed the influence of system parameters on the forming effect and put forward a criterion for the uniformity of tube forming [17]. Yu proposed that uniformity of tube forming depends on the ratio of the tube length to coil height [18]. Mo proposed an R-value criterion of tube uniformity through analyzing the electromagnetic tube expansion homogeneity at different aspect ratios [19].

In summary, innovated driving coils with different electromagnetic force distribution drive the rapid development of EMF. This paper is taking a step forward in investigating the feasibility of a concave coil to solve the issue of axial tube deformation. Feasibility studies using numerical and experimental Analyses are presented in [20]. Firstly, a new R-L criterion of homogeneity on deformation is proposed. Next, an electromagnetic-structural coupling model is established to analyze the relationship between the distribution of electromagnetic force generated by concave coils and the deformation homogeneity of the tube under various voltage levels. Finally, experimental measurements are carried out to assess the robustness of the proposed method.

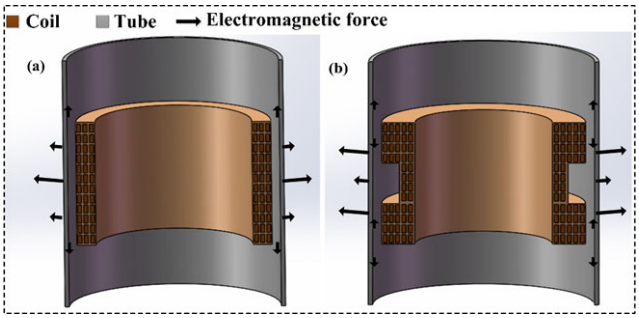

FIGURE 1. Coil structure and force distribution: (a) helix coil, (b) concave coil.

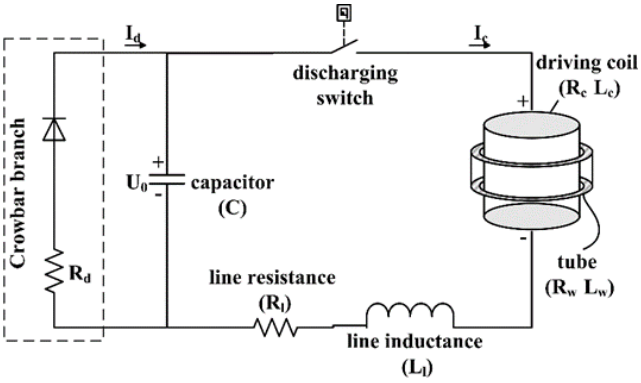

FIGURE 2. Schematic diagram of electromagnetic tube expansion system.

II. BASIC PRINCIPLE AND DESIGN

Due to the tube end effect, radial electromagnetic force is not distributed homogenously along the axial direction of the conventional electromagnetic tube expansion. This force is larger at the tube central area than the tube edges. This is due to the fact that, the tube edges are more restrained by the static region in the deformation process which eventually leads to the inhomogeneous deformation in the axial direction. To overcome this issue, a new concave coil structure is proposed in this paper. This coil can improve the forming quality of the tube by adjusting the distribution of the radial electromagnetic force as shown in Fig.1. By reducing the number of turns at the middle of the coil, the induced eddy current and magnetic flux density in this area will be reduced and hence the electromagnetic force exerted on the middle section of the tube will be weakened to improve the deformation homogeneity.

The EMF system mainly comprises charging system, capacitor power supply, discharging switch, driving coil and a tube as shown in the schematic diagram of Fig.2. A strong magnetic field is generated when the coil is driven by the capacitor discharging, which can drive the tube to accelerate and deform instantaneously.

The coupling relation between the driving coil and the tube is shown in Fig. 3. According to Faraday's law of

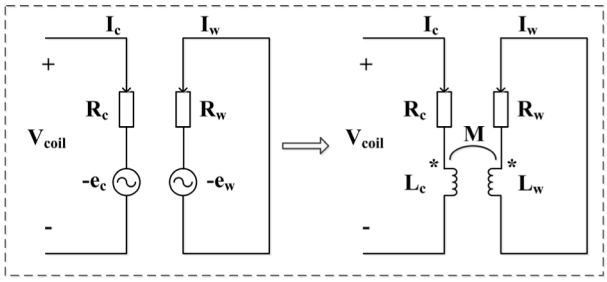

FIGURE 3. Coupling relationship between driving coil and tube.

electromagnetic induction, the following relations is held:

$$\begin{cases} e_{cc} = -L_c \dfrac{d\vec{I}_c}{dt} \\ e_{cw} = -M_{c-w} \dfrac{d\vec{I}_w}{dt} \end{cases} \tag{1}$$

$$\begin{cases} e_{ww} = -L_w \dfrac{d\vec{I}_w}{dt} \\ e_{wc} = -M_{w-c} \dfrac{d\vec{I}_c}{dt} \end{cases} \tag{2}$$

where I_c is the current of the driving coil and I_w is the induced eddy current of the tube. L_c and L_w are the self-inductance of the driving coil and the tube, respectively and M is the mutual inductance between the driving coil and the tube. e_{cc}, e_{ww} and e_{cw}, e_{wc} respectively represent the electromotive forces generated due to I_c and I_w.

The circuit is designed to facilitate the change of the waveforms of discharging current without affecting the forming efficiency through the use of a crowbar branch [21]. Therefore, the equivalent circuit of the electromagnetic tube expansion satisfies the following equations:

$$\left(R_l \vec{I_c} + L_l \frac{d\vec{I_c}}{dt}\right) + \left(R_c \vec{I_c} + L_c \frac{d\vec{I_c}}{dt} + M \frac{d\vec{I_w}}{dt}\right) = \vec{U_c} \tag{3}$$

$$\vec{U_c} = \vec{U_0} - \frac{1}{C} \int_0^t \left(\vec{I_c} + \vec{I_d}\right) dt \tag{4}$$

$$\begin{cases} \vec{I_d} = 0 & (U_c \geq 0) \\ \vec{I_d} = \dfrac{\vec{U_c}}{R_d} & (U_c < 0) \end{cases} \tag{5}$$

Ignoring the influence of the asymptotic line, the helix coil system can be seen as multiple closed rings in the axial direction. Then the structure of the electromagnetic field source, the coil system and the workpiece are all axially symmetric and can be simplified as a two-dimensional asymmetric model:

$$\nabla \times E_\phi = -\frac{\partial B_z}{\partial t} + \nabla \times (v_r \times B_z) \tag{6}$$

$$J_\varphi = \gamma E_\varphi \tag{7}$$

where E_Φ is the hoop component of the electric field intensity, B_z is the axial component of the magnetic flux density, v_r is the tube radial velocity, γ is the electrical conductivity, and J_Φ is the eddy current in the hoop direction.

Two terms on the right side of Eq. (6) represent the relationship of the curl of the induced electric field produced by the induced electromotive force and the motional electromotive force. The electromagnetic force on the tube is determined by the induced eddy current and flux density as below:

$$\begin{aligned} F_z &= J_\phi \times B_r \\ F_r &= J_\phi \times B_z \end{aligned} \tag{8}$$

Obviously, the distribution of the electromagnetic force is closely related to the magnetic flux density of the coil, and it is mainly dependent on the coil geometry. The force and displacement equation of the tube is given by the following equation:

$$\nabla \cdot \sigma + F = \rho \frac{\partial^2 u}{\partial t^2} \tag{9}$$

where σ is the stress tensor, F is the electromagnetic force density vector, ρ is the density of the tube, and u is the displacement vector.

The tube material used in this paper is AA6061-O, which can be simulated as Cowper-Symonds model. Its constitutive equation and quasi-static stress-strain curve can be expressed as below:

$$\sigma_{\text{ys}} = \begin{cases} E_{t\varepsilon} & \sigma_{\text{ys}} < \sigma_{\text{ys0}} \\ \sigma_{\text{ys0}} + A\varepsilon_{\text{pe}}^B & \sigma_{\text{ys}} \geq \sigma_{\text{ys0}} \end{cases} \tag{10}$$

$$\sigma = \left[1 + \left(\frac{\varepsilon_{pe}}{C_m}\right)^m\right] \sigma_{ys} \tag{11}$$

where E_t is the young's modulus, σ_{ys0} is the initial yield stress of the workpiece, ε_{pe} is the plastic strain that can be expressed as ε-(σ_{ys}/E). $A$and B are constants; 90.5 and 0.35 respectively. σ is the flow stress, m is the strain rate hardening parameter, C_m is the viscosity parameter.

The system parameters used in the simulation analysis are listed in Table 1.

A. FINITE ELEMENT MODEL

There is a strong coupling between the electromagnetic and structure fields in the electromagnetic tube expansion process. Finite element modeling is a reliable simulation tool to emulate physical process. A 2-D axial symmetry finite element model is developed using COMSOL software for the axis symmetry of electromagnetic force and tube deformation as shown in Fig. 4. The flowchart for the simulation process is shown in Fig. 5. The simulation includes four physical models: ''Circuit analysis model'' to calculate equations (3)–(5), ''Magnetic analysis model'' to calculate flux density, induced eddy current and electromagnetic force, ''Deformation analysis model'' to simulate the tube deformation behavior caused by the electromagnetic force, and ''Update mesh model'' for updating mesh elements with the deformation of the tube.

In order to verify the robustness of the simulated model, experimental measurements have been conducted and compared with the simulation results. For a discharging voltage

TABLE 1. Simulation parameters of the investigated system.

Symbol	Description	Value
Circuit		
C	Capacitance	320 μF
R_l	Line resistance	35 mΩ
L_l	Line inductance	15 μH
R_d	Resistance of Crowbar branch	150 mΩ
Workpiece		
D_W	Outer diameter	79 mm
h_W	Height	120 mm
T_W	Wall thickness	2 mm
ρ_w	Mass density	2700 kg/m^3
γ_w	Electrical conductivity	3.03e7 S/m
σ_{qs0}	Initial yield stress	32.6 MPa
v_w	Poisson ratio	0.33
E_w	Young modulus	70 GPa
Coil (conventional)		
D_{in}	Inter diameter	51.4 mm
D_{ou}	Outer diameter	67.4 mm
H_c	Height	52 mm
ρ_c	Mass density	8900 kg/m^3
γ_c	Electrical conductivity	5.98e7 S/m
v_c	Poisson ratio	0.35
E_c	Young modulus	118 GPa

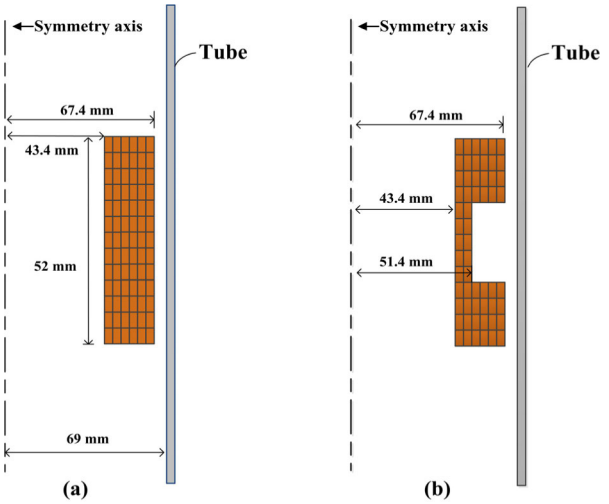

FIGURE 4. 2-D finite element model: (a) helix coil, (b) concave coil.

$U = 4.4$ kV, the generated current waveform obtained through simulation and experimental measurements is as shown in Fig. 6(a) which reveals a good agreement between the simulation and experimental results. Fig. 6(b) shows the corresponding deformation contour of the tube using simulation and practical measurements. In the simulation analysis, the diameter and height of the expanded tube are found to be 100.86mm and 112.44 mm respectively, which are very close to the experimental results (99.12 mm and 113.56 mm). The error between simulation and experimental data is less than 2% which reveals the accuracy of the developed finite element model.

B. R-L CRITERION FOR DEFORMATION HOMOGENEITY

It is more effective to analyze the tube deformation homogeneity after establishing a reasonable criterion for

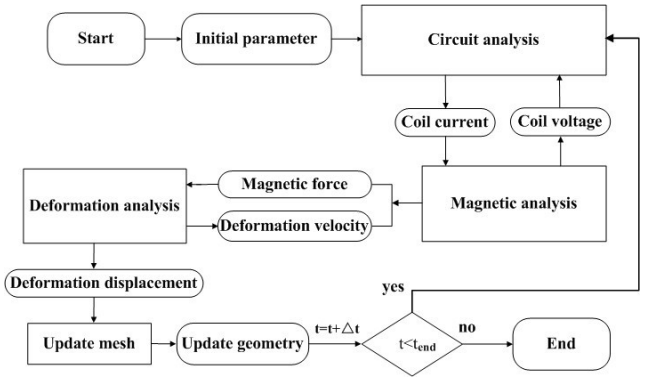

FIGURE 5. Flow chart of EMF simulation.

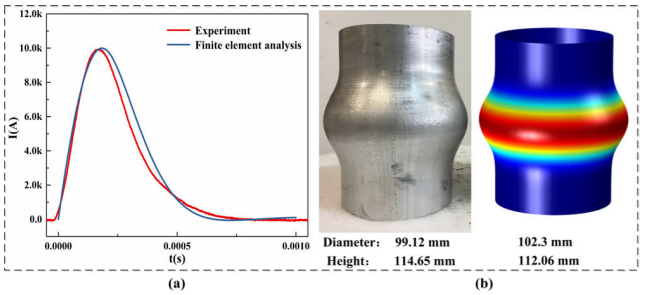

FIGURE 6. Simulation and experimental results: (a) coil current, (b) tube deformation.

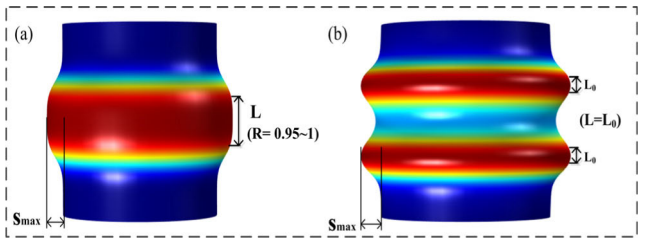

FIGURE 7. R-L criterion for deformation homogeneity.

deformation uniformity. Based on the R-value criterion presented in [19], this paper proposes a new R-L criterion of deformation uniformity for analyzing the deformation of the tube. The maximum displacement point S_{max} usually appears at the axial center of the tube and can be considered as a reference value whereas any displacement value S of any point along the axial direction is expressed as a ratio $R = \mathrm{S/S_{max}}$ that should be limited to a value in the range $0.95 \sim 1$. When this ratio reaches a critical value of 0.95, the corresponding point is recorded as the maximum displacement point of a length $L/2$ where L is the maximum deformation homogeneity range as shown in Fig. 7. The R-L criterion of deformation homogeneity is a direct method of uniformity. For similar tubes of the same material and height, the larger the value of L, the better the homogeneity on tube deformation.

C. ANALYSIS OF TUBE AXIAL UNIFORMITY

In order to validate the superiority of the proposed concave coil over the traditional helix coil currently used by the

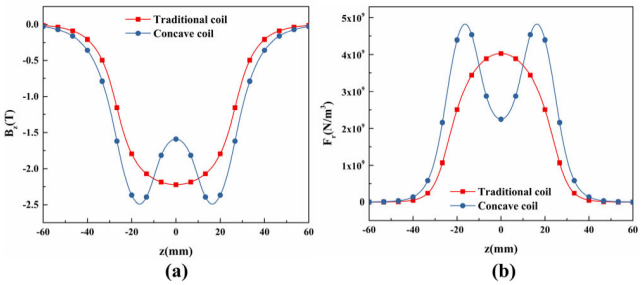

FIGURE 8. Performance of the two investigated coils (a) axial magnetic field density and (b) radial electromagnetic force distribution against tube displacement length (z).

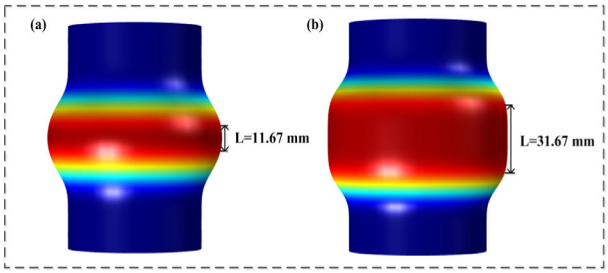

FIGURE 9. Tube homogeneity under the two investigated coils: (a) helix coil, (b) concave coil.

industry practice, the axial homogeneity of tube deformation based on both coils are compared and analyzed based on the geometrical parameter listed in Table 1.

Fig. 8 shows the axial magnetic field intensity and radial electromagnetic force distribution when each coil is employed. In contrary with the conventional helix coil and due to the decreased number of turns in the middle of the concave coil, the magnetic field density within the gap between the central section and the workpiece decreases accordingly. The reduction of the magnetic field density at the central section reforms the magnetic field profile to be in a concave shape as shown in Fig. 8(a). As the radial electromagnetic force mainly depends on the axial magnetic field density, the radial electromagnetic force will be also distributed in a concave shape in the axial direction as shown in Fig. 8(b). Results in Fig. 8(b) reveal that for the same tube displacement, the maximum radial electromagnetic force generated by the concave coil is greater than the force generated by conventional helix coil.

Fig. 9 shows tube homogeneity under the two investigated coils system. The discharge voltage in the conventional helix coil system is 3.37kV while it is 4.40kV in case of concave coil system. As previously shown in Fig.8, the radial electromagnetic force is distributed in a convex shape in the axial direction for the conventional helix coil system, which leads to inhomogeneous deformation in the axial direction. On the other hand, in case of concave coil system, the radial electromagnetic force is distributed axially in a concave shape and the displacement of the edges of the tube is increasing. According to R-L criterion of deformation homogeneity, the maximum homogeneous deformation range

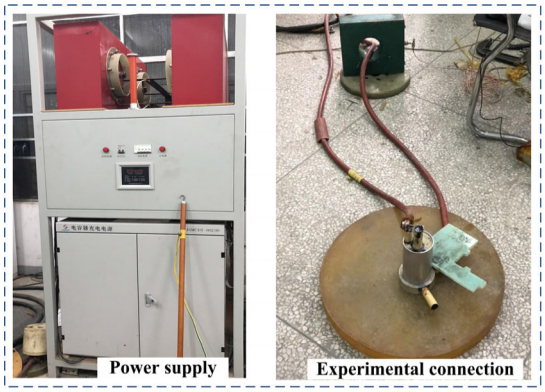

FIGURE 10. Part of the experimental setup.

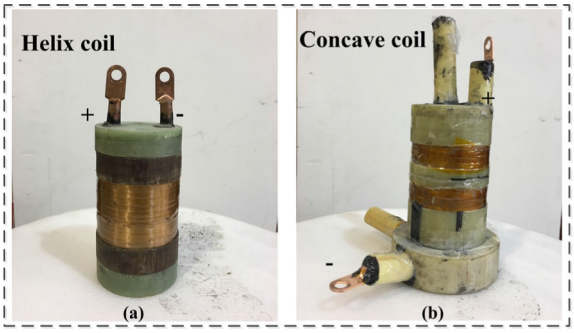

FIGURE 11. Design of the two investigated coils: (a) helix coil, (b) concave coil.

L is 11.67 mm and 31.67 mm for the helix coil system and the concave coil system, respectively. Figure 9 shows that the homogeneous deformation of the tube is significantly improved when the conventional helix coil is replaced by the proposed concave coil.

III. EXPERIMENTAL AND SIMULATION RESULTS

To validate the effectiveness of the homogeneous deformation of the tube using the proposed concave coil, experimental measurements are carried out at Wuhan National High Magnetic Field Center as shown in the part of the hardware setup in Fig. 10. The power supply in Fig. 10 consists of two capacitors of 320 μF total capacitance, maximum charging voltage of 25 kV and maximum discharging energy of 200 kJ. In order to simplify the fabrication of the experimental coils, the structures of the two investigated coils are designed as shown in Fig. 11. The two coils are made of copper wire of rectangular cross-section of 1 $\times$ 4 mm^2 with Zylon-reinforced external layer. The tube is made of Aluminum alloy AA6061-O. Schematic diagram of the experimental setup is shown in Fig. 12.

When a 5.4 kV discharging voltage is applied to the conventional helix coil, the maximum deformation of the tube is found to be the same when a 6.5 kV is applied to the concave coil with a shape of the expanded tube as shown in Fig. 13. The value of L is 7.87 mm in case of conventional coil and 27.22 mm when the concave coil is used, which is 3.46 times of the former. Apparently, the radial electromagnetic force

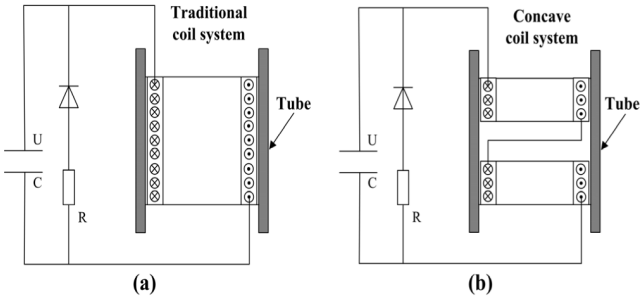

FIGURE 12. Schematic diagram of the experimental setup (a) conventional helix coil, (b) concave coil.

FIGURE 13. Photos of the Expanded tube after discharging with a system of helix coil and concave coil.

generated by the concave coil can greatly improve the homogeneous deformation of the tube.

The relationship between electromagnetic force distribution and deformation homogeneity is further investigated by changing the discharging voltage as elaborated below.

Results show that the two peaks of the radial electromagnetic force increase when the discharging voltage gradually increases from 3.6 kV to 5.4 kV. A further increase in the discharging voltage results in altering the deformation of the tube from concave to convex profile. This proves that forming results are sensitive to the discharging voltage especially at high voltage levels as the deformation tube profile is being similar to the deformation effect when a conventional helix coil is employed as shown in Fig. 14 (b). The discharging voltage effect on the electromagnetic force acting on the workpiece is directly affecting the forming process.

Fig.14 (c) shows the maximum deformation homogeneity range of the tube at different discharging voltage levels. Results show that the maximum deformation homogeneity range increases with the increase of the discharging voltage level up to 4.4 kV after which it decreases. As shown in Fig. 14 (c), the value of L increases and reaches a maximum value that is corresponding to a critical transition point from concave to convex profile at a voltage level of 4.4 kV. With the further increase of the discharging voltage, the value of L decreases and the tube is converted to a convex profile shape. The above results reveal that discharging voltage level has a great influence on the deformation homogeneity of the tube

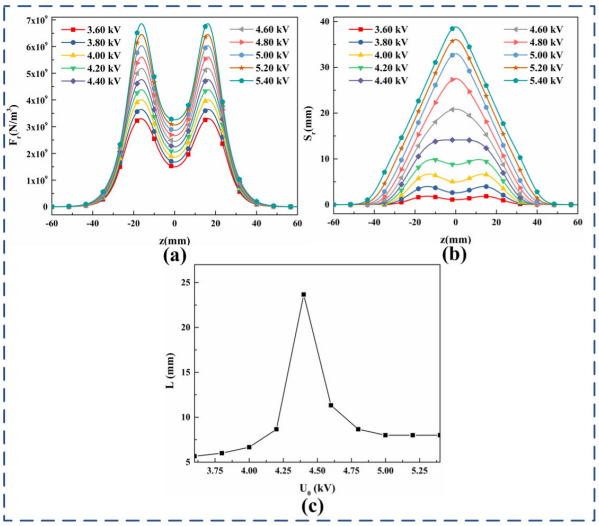

FIGURE 14. Effect of discharging voltage: (a) radial electromagnetic force distribution, (b) radial displacement, (c) deformation homogeneity range for a concave coil system.

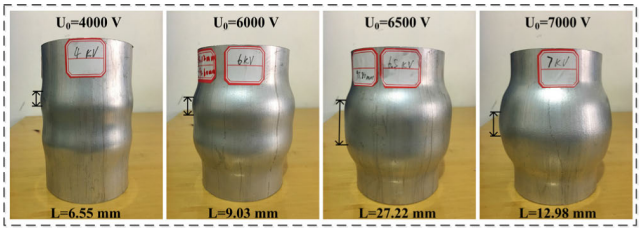

FIGURE 15. Experimental measurements for the effect of discharging voltage on the deformation homogeneity of the tube.

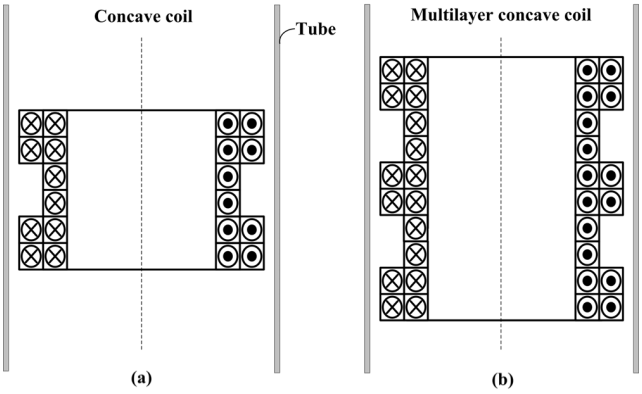

FIGURE 16. Concave coil structure (a) conventional structure (b) multi-layer structure.

in the axial direction, and there exists a critical discharging voltage level where the tube exhibits a maximum deformation homogeneity range.

To validate the effect of discharging voltage on deformation homogeneity of the tube, a series of experiments were carried out with the simplified concave coil shown in Figure 10. The expanded tube under different discharging voltage levels is shown in Fig. 15. Experimental results indicate that the value of L increases with the increase in the discharging voltage level from 4 kV to 6.5 kV. When the

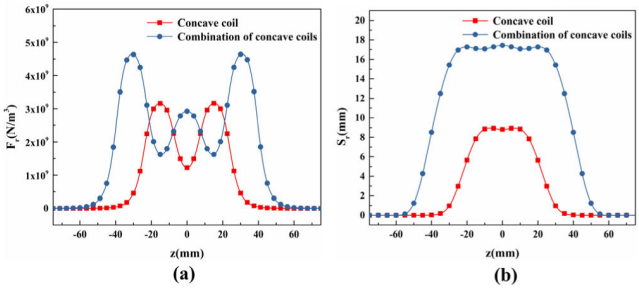

FIGURE 17. Performance of the conventional and multilayer concave coil (a) axial electromagnetic force distribution, (b) radial displacement of the expanded tube.

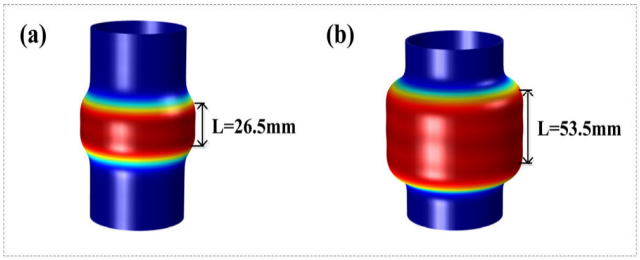

FIGURE 18. Finite element simulation results of *L* (a) concave coil (b) multilayer concave coil.

discharging voltage level reaches about 7 kV, the value of L decreases and the tube deformation shape is turning to a convex profile, which agrees well with the simulation results above. Experimental results show that the critical discharging voltage level of the used tube is 6.5 kV with a maximum deformation homogeneity range of 27.22 mm.

IV. ANALYSIS OF MULTILAYER CONCAVE COIL

To investigate the axial homogeneous deformation of a long tube, a multilayer concave coil as shown in Fig. 16 is introduced to further increase the tube deformation homogeneity range.

Fig. 17(a) shows the radial electromagnetic force distribution under the conventional concave coil and multilayer concave coil. It can be observed that the number of peaks of the radial electromagnetic force has increased from two, in case of conventional concave coil, to three in case of multilayer concave coil. Fig.17 (b) shows the radial displacement of the expanded tube with the maximum deformation homogeneity range for the two coils. It can be seen that the depth and length of the expanded tube increase significantly when a multilayer concave coil is employed. As shown in Fig. 18, the corresponding simulation results of L are found to be 23.75 mm in case of conventional concave coil and 51.66 mm when a multilayer structure for the proposed concave coil is adopted.

V. CONCLUSION

This paper investigates the electromagnetic tube expansion with concave and helix coils. Simulation and experimental analyses have been conducted to explore the homogeneity on tube deformation under these two coils. The following conclusions can be drawn from the obtained results:

- By comparison, the radial electromagnetic force generated by the concave coil can greatly improve the homogeneous deformation of the tube than the conventional helix coil. In the investigated case in this paper, the maximum deformation homogeneity range increased from 11.667 mm in case of helix coil to 31.666 mm in case of concave coil.
- With the increase in the discharging voltage, the forming deformation of the tube changes from concave to convex profile at certain critical discharging voltage. At this critical discharging voltage level, the tube exhibits maximum deformation homogeneity range.
- The application of multilayer concave coil can further increase the maximum deformation homogeneity range. This is expected to be a new solution to solve the axial homogeneous deformation of long tubes.

REFERENCES

[1] V. Psyk, D. Risch, B. L. Kinsey, A. E. Tekkaya, and M. Kleiner, "Electromagnetic forming—A review," *J. Mater. Process. Technol.*, vol. 211, no. 5, pp. 787–829, May 2011.

[2] Q. Xiong, H. Tang, C. Deng, L. Li, L. Qiu, "Electromagnetic attraction-based bulge forming in small tubes: Fundamentals and simulations," *IEEE Trans. Appl. Supercond.*, vol. 28, no. 3, Apr. 2018, Art. no. 0600505.

[3] L. Qiu, Y. Xiao, C. Deng, Z. Li, Y. Xu, Z. Li, and P. Chang, "Electromagnetic-structural analysis and improved loose coupling method in electromagnetic forming process," *Int. J. Adv. Manuf. Technol.*, vol. 89, nos. 1–4, pp. 701–710, Mar. 2017.

[4] Q. Cao, Z. Li, Z. Lai, Z. Li, X. Han, and L. Li, "Analysis of the effect of an electrically conductive die on electromagnetic sheet metal forming process using the finite element-circuit coupled method," *Int. J. Adv. Manuf. Tech.*, vol. 101, nos. 1–4, pp. 549–563, Mar. 2019.

[5] M. Kamal and G. S. Daehn, "A uniform pressure electromagnetic actuator for forming flat sheets," *J. Manuf. Sci. Eng.*, vol. 129, no. 2, pp. 369–379, Oct. 2007.

[6] S. Golowin, M. Kamal, J. Shang, J. Portier, A. Din, G. S. Daehn, J. R. Bradley, K. E. Newman, S. Hatkevich, "Application of a uniform pressure actuator for electromagnetic processing of sheet metal," *J. Mater. Eng. Perform.*, vol. 16, no. 4, pp. 455–460, Aug. 2007.

[7] M. Kamal, J. Shang, V. Cheng, S. Hatkevich, and G. S. Daehn, "Agile manufacturing of a micro-embossed case by a two-step electromagnetic forming process," *J. Mater. Process. Technol.*, vol. 190, nos. 1–3, pp. 41–50, Jul. 2007.

[8] C. Weddeling, M. Hahn, G. S. Daehn, and A. E. Tekkaya, "Uniform pressure electromagnetic actuator —An innovative tool for magnetic pulse welding," *Procedia CIRP*, vol. 18, pp. 156–161, Jun. 2014.

[9] K. Kiliclar, O. K. Demir, I. N. Vladimirov, L. Kwiatkowski, A. Brosius, S. Reese, and A. E. Tekkaya, "Combined simulation of quasi-static deep drawing and electromagnetic forming by means of a coupled damage-viscoplasticity model at finite strains," presented at the 5th Int. Conf. High Speed Forming, Dortmund, Germany, May 2012.

[10] M. Ahmed, S. K. Panthi, N. Ramakrishnan, A. K. Jha, A. H. Yegneswaran, and R. Dasgupta, "Alternative flat coil design for electromagnetic forming using FEM," *Trans. Nonferrous Metals Soc. China*, vol. 21, no. 3, pp. 618–625, Mar. 2011.

[11] L. Qiu, Y. Yu, Y. Yang, X. Nie, Y. Xiao, Y. Ning, F. Wang, and C. Cao, "Analysis of electromagnetic force and experiments in electromagnetic forming with local loading," *Int. J. Appl. Electrom.*, vol. 57, no. 1, pp. 29–37, Apr. 2018.

[12] Q. Cao, L. Du, Z. Li, Z. Lai, Z. Li, M. Chen, X. Li, S. Xu, Q. Chen, X. Han, and L. Li, "Investigation of the Lorentz-force-driven sheet metal stamping process for cylindrical cup forming," *J. Mater. Process. Technol.*, vol. 271, pp. 532–541, Mar. 2019.

[13] J. Zhao, J. H. Mo, X. H. Cui, and L. Qiu, "Research on numerical simulation and forming uniformity of electromagnetic incremental tube bulging," *J. Plasticity Eng. China*, vol. 19, no. 5, pp. 92–99, Oct. 2012.
[14] A. Vivek, K.-H. Kim, and G. S. Daehn, "Simulation and instrumentation of electromagnetic compression of steel tubes," *J. Mater. Process. Technol.*, vol. 211, no. 5, pp. 840–850, May 2011.
[15] S. K. Dond, M. R. Kulkarni, S. Kumar, P. C. Saroj, and A. Sharma, "Magnetic field enhancement using field shaper for Electromagnetic welding system," in *Proc. IEEE Appl. Electromagn. Conf. (AEMC)*, Dec. 2015, pp. 1–2.
[16] L. Qiu, Y. Yu, Z. Wang, Y. Yang, Y. Yang, and P. Su, "Analysis of electromagnetic force and deformation behavior in electromagnetic forming with different coil systems," *Int. J. Appl. Electromagn. Mech.*, vol. 57, no. 3, pp. 337–345, Jun. 2018.
[17] Z. Li, C.-F. Li, and Z.-H. Zhao, "Transient distribution of magnetic pressure in electromagnetic tube bulging," *Mater. Sci. Tech.*, vol. 16, no. 3, pp. 301–305, Jun. 2008.
[18] H.-P. Yu, C.-F. Li, D.-H. Liu, and X. Mei, "Tendency of homogeneous radial deformation during electromagnetic compression of aluminium tube," *Trans. Nonferrous Met. Soc. China*, vol. 20, no. 1, pp. 7–13, Jan. 2010.
[19] F. Q. Li, Y. Fang, Y. Zhu, J. H. Mo, and J. J. Li, "Study on the homogeneity of deformation under electromagnetic expansion of metal tube," *Int. J. Appl. Electrom. Mech.*, vol. 42, no. 1, pp. 13–25, Jan. 2013.
[20] L. Qiu, Y. Yu, Q. Xiong, C. Deng, Q. Cao, X. Han, and L. Li, "Analysis of electromagnetic force and deformation behavior in electromagnetic tube expansion with concave coil based on finite element method," *IEEE Trans. Appl. Supercond.*, vol. 28, no. 3, Apr. 2018, Art. no. 0600705.
[21] Q. Cao, X. Han, Z. Lai, Q. Xiong, X. Zhang, Q. Chen, H. Xiao, and L. Li, "Analysis and reduction of coil temperature rise in electromagnetic forming," *J. Mater. Process. Technol.*, vol. 225, pp. 185–194, Nov. 2015.

LI QIU (M'18) received the B.S., M.S., and Ph.D. degrees in electrical engineering from the Huazhong University of Science and Technology, Wuhan, China, in 2012.

He is currently an Associate Professor with the College of Electrical Engineering and New Energy, China Three Gorges University, Yichang. He is the author of more than 15 articles and more than ten inventions. His research interests include technology of pulsed high magnetic field, high-voltage technology, and electromagnetic forming. He is also a Periodical Reviewer of the IEEE TRANSACTIONS ON APPLIED SUPERCONDUCTIVITY and *International Journal of Applied Electromagnetics and Mechanics*.

YANTAO LI is currently pursuing the degree in electrical engineering with the College of Electrical Engineering and New Energy, China Three Gorges University, Yichang.

YIJIE YU received the M.S. degree in electrical engineering from the College of Electrical Engineering and New Energy, China Three Gorges University, Yichang. He is currently with State Grid Putian Electric Supply Company, Fujian.

A. ABU-SIADA (M'07–SM'12) received the B.Sc. and M.Sc. degrees in electrical engineering from Ain Shams University, Egypt, in 1998, and the Ph.D. degree in electrical engineering from Curtin University, Australia, in 2004, where he is currently an Associate Professor and the Discipline Lead of the Department of Electrical and Computer Engineering. His research interests include power electronics, power system stability, condition monitoring, and power quality. He is also the Vice-Chair of the IEEE Computation Intelligence Society and the WA Chapter. He is also the Editor-in-Chief of the *International Journal of Electrical and Electronic Engineering* and a regular Reviewer of various IEEE Transactions.

QI XIONG (M'18) received the B.S., M.S., and Ph.D. degrees in electrical engineering from the Huazhong University of Science and Technology, Wuhan, China, in 2016.

He is currently a Lecturer with the College of Electrical Engineering and New Energy, China Three Gorges University, Yichang. His research interests include technology of pulsed high magnetic field, high-voltage technology, and electromagnetic forming.

XIAOXIANG LI is currently pursuing the Ph.D. degree in electrical engineering with the Huazhong University of Science and Technology, Wuhan, China.

LIANG LI graduated from the Electrical Engineering College, Huazhong University of Science and Technology (HUST), in 1985. He received the master's degree in fusion engineering from the Plasma Physics Institute, Chinese Academy of Science, in 1988, and the master's and Ph.D. degrees from Katholieke University Leuven (KU Leuven), Belgium, in 1992 and 1997, respectively. He completed his postgraduate study at the Plasma Physics Institute, Chinese Academy of Science.

From 1997 to 2000, he was an Associate Researcher with the National High Magnetic Field Laboratory (NHMFL) leading the pulsed magnet development for the Los Alamos National Laboratory. In 2000, he joined the Superconducting and Electromagnetics Lab, Global Research Center, GE Company, Niskayuna, NY, USA, as a Senior Electrical Engineer. Since 2007, he has been the General Manager and the Chief Engineer of the National Major Science and Technology Infrastructure Project and the Pulsed High Magnetic Field Facility Project of the HUST, respectively.

PAN SU received the M.S. degree in electrical engineering from the College of Electrical Engineering and New Energy, China Three Gorges University, Yichang. He is currently with the College of Electrical Engineering and New Energy, China Three Gorges University.

QUANLIANG CAO received the B.S., M.S., and Ph.D. degrees in electrical engineering from the Huazhong University of Science and Technology, Wuhan, China, in 2013, where he is currently an Associate Research Fellow with the Wuhan National High Magnetic Field Center.

He is the author of more than 19 articles and more than six inventions. His research interests include magnetic manipulation of micro/nanoparticles and electromagnetic forming. He is also a Periodical Reviewer of the IEEE TRANSACTIONS ON MAGNETICS, IEEE ACCESS, *Sensors and Actuators B: Chemical*, and *Microfluidics and Nanofluidics*.